

Fast Synthesis of Metal-incorporated NKX-2 (MeNKX-2) Using Novel Ionic Liquid *via* Ionothermal Approach

Jia Pei Ghoi and Eng-Poh Ng*

School of Chemical Sciences, Universiti Sains Malaysia, 11800 USM, Penang, Malaysia

*Corresponding author (e-mail: epng@usm.my)

The incorporation of other metal and non-metal cations into the aluminophosphate (MeAlPO-*n*) molecular sieves has played a major role in enhancing their applications in the field of adsorption, separation, the formation of host-guest advanced materials and catalysis. These materials are usually synthesized under hydrothermal condition. Recently, the ionothermal method has been reported as a green synthesis approach for the synthesis of aluminophosphate (AlPO-*n*) and metalloaluminophosphate (MeAlPO-*n*) materials by using non-volatile ionic liquids as a solvent and a structure directing agent. In this work, ionothermal synthesis of metastable metal-incorporated aluminophosphate NKX-2 (MeNKX-2), where Me = Zr, Cr, Co and Fe) using 1-benzyl-2,3-dimethylimidazolium chloride, [bdmim]Cl new ionic liquid was reported. The ionic liquid was first prepared and characterized before use for the synthesis of molecular sieves. The synthesized MeNKX-2 series were then characterized by X-ray diffraction, Fourier transform-infrared spectroscopy, scanning electron microscopy coupled with energy dispersive X-ray spectroscopy and ultraviolet-visible spectroscopy. The analyses revealed that MeNKX-2 could be synthesized in a fast and convenient way and the crystals with unique morphology could be obtained within 20 min instead of several days under hydrothermal condition.

Key words: Metal-incorporated NKX-2; ionic liquid; ionothermal synthesis; microporous materials; zeolites

Received: October 2015; Accepted: September 2016

The discovery of aluminophosphate (AlPO-*n*) made by Wilson *et al.* in 1982 is considered as a milestone in the development of molecular sieve materials [1]. These molecular sieves have drawn considerable attentions due to their framework structures that closely resemble zeolite topologies [1,2]. Typically, these zeotype materials are prepared under the hydrothermal condition at an elevated temperature in the presence of organic template [2,3]. Recently, a new method called ionothermal synthesis has been reported [4]. Unlike hydrothermal method, this technique uses the ionic liquid as a reaction solvent and as a structure-directing agent. The most important features of this strategy are the use of green ionic liquid instead of harmful quaternary ammonium hydroxides, and the synthesis can be performed

in an open vessel instead of using autoclave due to the low vapor pressure of the ionic liquids. In comparison with the hydrothermal pathway, the crystallization process in ionic-liquid-mediated synthesis is different since the reaction takes place in an ionic environment (merely cations and anions) whereas the solvent used in the hydrothermal method is predominantly molecular. Moreover, as the solvent can also act as a template; there is no competition between template-framework and solvent-framework during ionothermal synthesis. Thus, this gives better control on the reaction [4].

Classically, phosphoric acid (H₃PO₄) is used as a phosphorus source in the synthesis of AlPO-*n* microporous materials. However, phosphorus acid (H₃PO₃) as a new phosphorus source has also

been reported [5–7]. H_3PO_3 is described with the structural formula $\text{HPO}(\text{OH})_2$ where this species exists in equilibrium with a $\text{P}(\text{OH})_3$ tautomer. Due to the rapid interconversion, these tautomers alter the charge of P species in the framework (P^{3+} or P^{5+}). Also, H_3PO_3 exhibits different behaviours compare with H_3PO_4 during the crystallization of aluminophosphate due to its dibasic acid character ($\text{pK}_{a1} = 1.80$, $\text{pK}_{a2} = 6.15$) [8]. As a result, the synthesis reproducibility is enhanced and the resulting materials through this route give different and improved catalytic properties [7,9,10]. Hence, the use of H_3PO_3 enables exploration of metastable intermediate phase with novel open-framework crystalline phase and unique framework properties.

The introduction of transition metals into the framework of aluminophosphate molecular sieves (MeAPO-*n*) is a useful method to modify the properties of the materials, enabling their applications in catalysis, adsorption, etc. However, the effect of transition metals on the crystallization process of MeAPO-*n* in ionic liquid media is still not clear, and hence an attempt to study this effect if it is worthy of academic pursuit.

In the present work, the formation of metal-incorporated NKX-2 (MeNKX-2) is studied under ionothermal condition using H_3PO_3 as a phosphorous source. The crystallization process was carried out at 180°C using a new ionic liquid, *viz.* 1-benzyl-2,3-dimethylimidazolium chloride, [bdmim]Cl.

EXPERIMENTAL

Synthesis of 1-benzyl-2,3-dimethylimidazolium Chloride, [bdmim]Cl

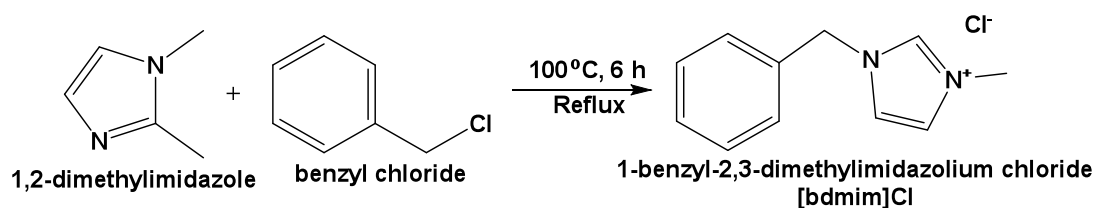
The [bdmim]Cl ionic molten salt was prepared as follows: 1,2-dimethylimidazole (45.00 g, 96%, Merck) was dissolved in ethanol (40 ml, 99.7%, QRëc) in a 250 ml round bottom flask. Then, benzyl chloride (86 ml, 99%, Merck) was added to the mixture. The resulting solution was refluxed at 100°C for 6 h before the round bottom flask was cooled down in an ice bath to allow white crystals to precipitate out (Scheme 1). The white crystals were purified and washed

with acetone prior to drying in an oven at 100°C overnight. The pure ionic molten salt was kept in a tight propylene bottle and stored in a desiccator. Product yield 86.4%. ^1H NMR (400 MHz, ppm, D_2O) appears as follows: $\delta = 2.48$ (3H, imidazole N-C (CH_3)-N), 3.70 (3H, imidazole N- CH_3), 5.28 (2H, imidazole N- CH_2 - C_6H_5), 7.22 (1H, imidazole N- $\text{CH}=\text{CH}$ -N), 7.24 (1H, imidazole N- $\text{CH}=\text{CH}$ -N) and 7.28–7.41 (5H, phenyl). FT-IR (KBr disk) cm^{-1} : 1026 (imidazolium, C-N), 1452 and 1643 (aromatic C=C), 1532 (imidazolium, C=N), 3411 (O-H stretching). Anal. calcd for $\text{C}_{12}\text{H}_{15}\text{N}_2\text{Cl}$: C, 64.72%; H, 6.79%; N, 12.58%; Cl, 15.92%; found: C, 65.03%; H, 6.66%; N, 11.55%; Cl, 16.77%.

Ionothermal Synthesis of Metal-incorporated NKX-2 (MeNKX-2)

The aluminum and phosphorus sources were aluminum isopropoxide ($\text{Al}[\text{OCH}(\text{CH}_3)_2]_3$) and H_3PO_3 , respectively. Initially, a H_3PO_3 solution (85 wt% in water) was first prepared. ZrCl_4 (98%), $\text{CrCl}_3 \cdot 6\text{H}_2\text{O}$ (96%), $\text{CoCl}_2 \cdot 6\text{H}_2\text{O}$ (95%) and $\text{FeCl}_3 \cdot 6\text{H}_2\text{O}$ (98%) were used as the sources of zirconium, chromium, cobalt, and iron, respectively. MeNKX-2 was synthesized from a gel with a molar composition of 1.0 Al_2O_3 : 3.0 P_2O_3 : 40 [bdmim]Cl: 5.76 H_2O : 0.065 Me (Me = metal).

The synthesis procedure was as follows. The metal sources were first put into 15 ml Teflon-lined stainless steel autoclaves. Phosphorus acid (0.495 g, H_3PO_3 , 85%, Mallinckrodt) was added dropwise under stirring until all the metal sources had dissolved into it. Then, aluminum isopropoxide (0.416 g, $\text{Al}[\text{OCH}(\text{CH}_3)_2]_3$, 98%, Aldrich) and [bdmim]Cl ionic molten salt (8.89 g) were added into the Teflon-lined stainless steel autoclaves. All Teflon-lined stainless steel autoclaves were sealed and heated in an oven at 180°C and kept for 10, 20 and 30 min for crystallization. The Teflon-lined stainless steel autoclaves were taken out from the oven and cooled to room temperature. The solid products were recovered by centrifugation (8500 rpm, 10 min), washed with distilled water and acetone for several times. The solid products were dried at 100°C overnight.



Scheme 1. Synthesis of [bdmim]Cl ionic molten salt.

Characterization

[bdmim]Cl ionic molten salt. [bdmim]Cl ionic liquid was characterized by using a Bruker Ultrashield 400 spectrometer with tetramethylsilane as a standard and D₂O as a solvent. Chemical analyses were performed on a Perkin Elmer 2400 Series II CHNS/O analyzer to determine the constituent of elements in of [bdmim]Cl. The functional groups in pure [bdmim]Cl ionic salt were determined with a Perkin Elmer's System 2000 IR spectrometer using the NaCl pellet technique (NaCl: sample weight ratio = 150: 1).

Metal-incorporated NKX-2 (MeNKX-2). Powder XRD patterns were recorded on a PANalytical X'Pert PRO diffractometer with Cu K_α radiation ($\lambda = 0.15418$ nm, 40 mA, 45 kV, step size of 0.02° and a scan speed of 0.2°/min). The morphology of the samples was analyzed by a Leo Supra 50VP field emission scanning electron microscope (FESEM) operating at 30 kV. The FTIR spectra were obtained with a Perkin Elmer's System 2000 IR spectrometer using NaCl pellet technique. The UV-Vis spectra were measured in the spectral range 320–900 nm using a Varian Cary® 100 UV-VIS-NIR spectrophotometer.

RESULTS AND DISCUSSION

Previously, aluminophosphate NKX-2 was hydrothermally synthesized at 180°C for 2–5 days [11]. Shi *et al.* synthesized aluminophosphate NKX-2 ionothermally by using 1-ethyl-2,3-dimethylimidazolium bromide (EMMIMBr) as the ionic liquid and the formation of NKX-2 can be achieved in 3 h under an open vessel condition [12]. On the other hand, Gómez-Hortigüela *et al.* described the synthesis of AlPO-5 and SAPO-5

materials (AFI topology) using tertiary amines or quaternary ammonium ions containing one or two benzyl rings as structure-directing agents (SDA) and found that both templates containing mono and dibenzyl functional groups show a high space-filling ability in AFI pore framework [13]. This allows us to make an assumption that crystallization of metal incorporated aluminophosphate NKX-2 (MeNKX-2) by using [bdmim]Cl as a SDA will be successful.

The development and structure formation of MeNKX-2 crystals via ionothermal synthesis were evaluated and followed by XRD and IR spectroscopy analyses. The XRD patterns of solid products obtained after 10, 20 and 30 min of heating was shown (Figure 1). Initially, no crystalline solid was formed after 10 min (Figure 1a). When the heating period was prolonged to 20 min, several peaks ($2\theta = 12.9^\circ, 25.8^\circ, 29.0^\circ$ and 33.9°) which were assigned to MeNKX-2 appeared [12]. When the heating period was prolonged to 30 min, the diffraction peaks were becoming more intense and resolve (Figure 1c). No impurity was found which could be confirmed by the absence of extra XRD peaks.

The MeNKX-2 products were characterized with the FT-IR spectroscopy to study the effect of heating time on the formation of MeNKX-2 crystals. The IR spectra of solid products obtained after 10 and 20 min of heating were shown (Figure 2). As can be seen, the IR pattern of the solids heated for 10 min was different from that of NKX-2 (Figure 2a). After heating the solids for another 10 min, the pattern in the fingerprint region change significantly indicating the transformation had been occurred in the solid product (Figure 2b). As shown, the IR pattern of MeNKX-2 was similar to that of pure NKX-2 [12]. The bands at 1036 and

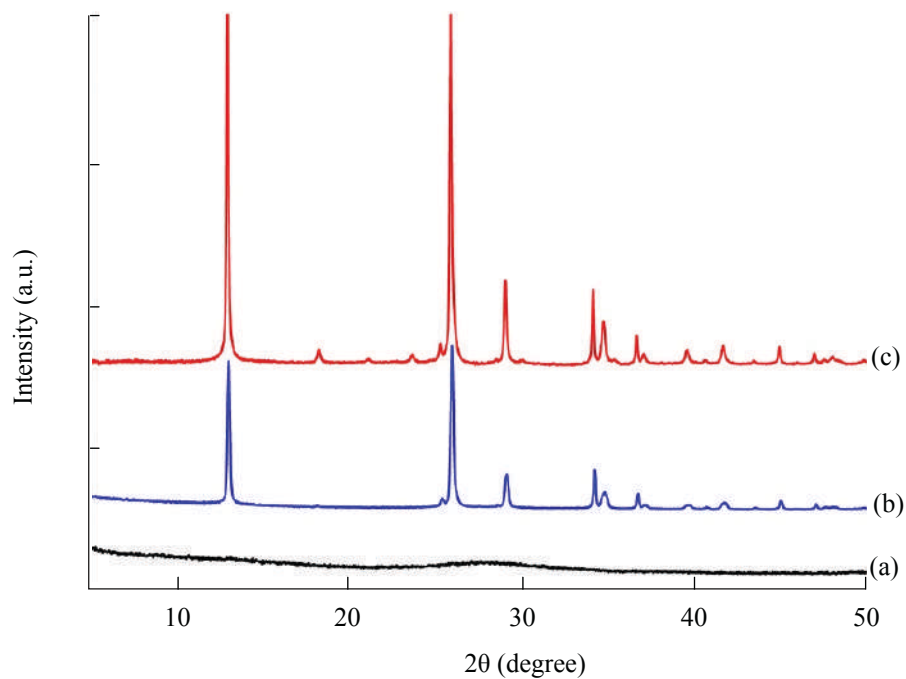


Figure 1. XRD patterns of MeNKX-2 synthesis by using (a) 10 min, (b) 20 min and (c) 30 min. The solid products were obtained with a molar composition of $1.0\text{Al}_2\text{O}_3 : 3.0\text{P}_2\text{O}_5 : 40[\text{bdmim}]\text{Cl} : 5.76\text{H}_2\text{O} : 0.065\text{Me}$ (Me = Zr, Cr, Co and Fe) at 180°C .

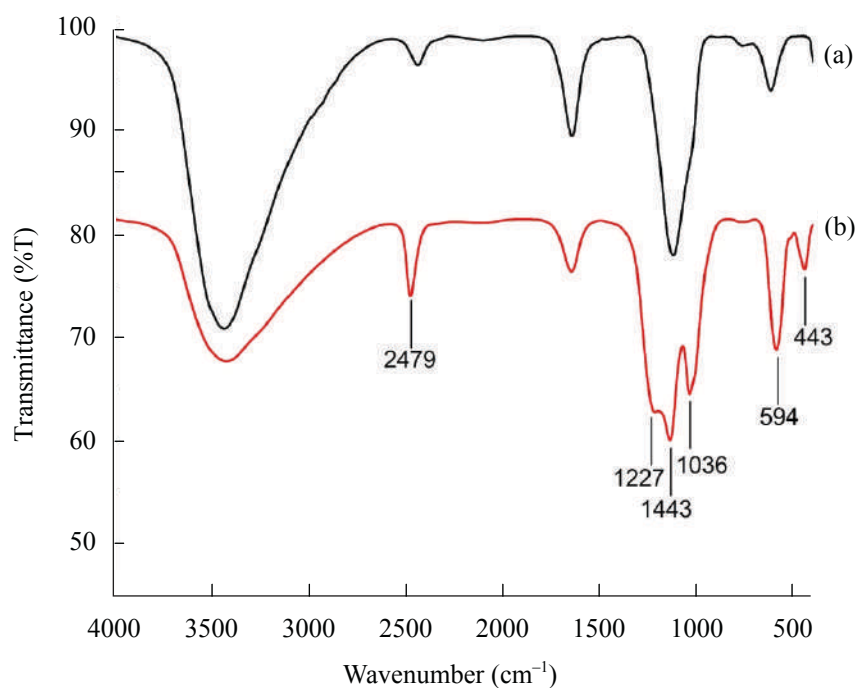


Figure 2. FT-IR spectra of MeNKX-2 solids after (a) 10 min and (b) 20 min of heating.

2479 cm^{-1} were attributed to P-H deformation and P-H stretching mode of HPO_3^{2-} , respectively. The two bands at 1143 and 1227 cm^{-1} were assigned to the P-O asymmetric stretching modes while the bands in the region of 400–600 cm^{-1} were due to the T-O-T vibration modes (T = Al, P) [12].

The effect of the introduction of transition metals during the crystallization of NKX-2 was also studied by using XRD technique. Figure 3 shows the XRD patterns of NKX-2 and MeNKX-2 solid products obtained after 20 min of ionothermal heating using molar composition of $1.0\text{Al}_2\text{O}_3$: $3.0\text{P}_2\text{O}_5$: $40[\text{bdmim}]\text{Cl}$: $5.76\text{H}_2\text{O}$: 0.065Me and $1.0\text{Al}_2\text{O}_3$: $3.0\text{P}_2\text{O}_5$: $40[\text{bdmim}]\text{Cl}$: $5.76\text{H}_2\text{O}$, respectively. The XRD data showed that without adding any transition metal, the solid consisted of amorphous (dominant phase) and NKX-2 phases was obtained. In contrast, pure and fully crystalline phase of MeNKX-2 was crystallized upon the addition of transition metals. Hence, it indicated the positive effect of transition metals in enhancing the crystallization rate of NKX-2 solid.

UV-Vis Spectroscopy Analysis of MeNKX-2

The ultraviolet-visible spectroscopy was used to investigate the incorporation of transition metals into the NKX-2 framework. Figure 4 shows the UV-Vis spectra of MeNKX-2 solid products obtained after 20 min of heating. As can be seen, the band at 214 nm was assigned to the oxygen to metal ion charge transition in the monoatomic dispersed metal ion in the framework [14]. For CrNKX-2, the band at 260 nm was due to the $\text{O} \rightarrow \text{Cr}$ (VI) charge transfer transitions of chromate or polychromate species [15]. For FeNKX-2, the band at 248 nm was due to the iron species converted to tetrahedral framework iron during crystallization. Also, the band at 274 nm for ZrNKX-2 and FeNKX-2 was the characteristic band of highly isolated six-coordinated Fe^{3+} and Zr^{2+} complexes [14]. For CoNKX-2, the band at 242 nm was due to the oxygen to metal charge transfer whereas the band at 280 nm was due to the cobalt in octahedral environment [16].

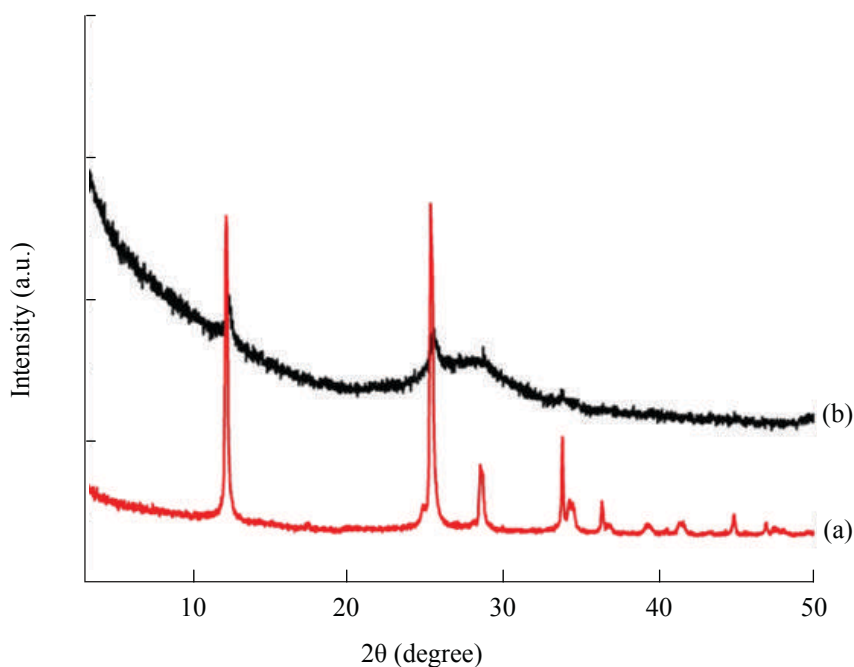


Figure 3. XRD patterns of (a) NKX-2 and (b) MeNKX-2. The solid products were obtained with the molar compositions of $1.0\text{Al}_2\text{O}_3$: $3.0\text{P}_2\text{O}_5$: $40[\text{bdmim}]\text{Cl}$: $5.76\text{H}_2\text{O}$: 0.065Me and $1.0\text{Al}_2\text{O}_3$: $3.0\text{P}_2\text{O}_5$: $40[\text{bdmim}]\text{Cl}$: $5.76\text{H}_2\text{O}$, respectively.

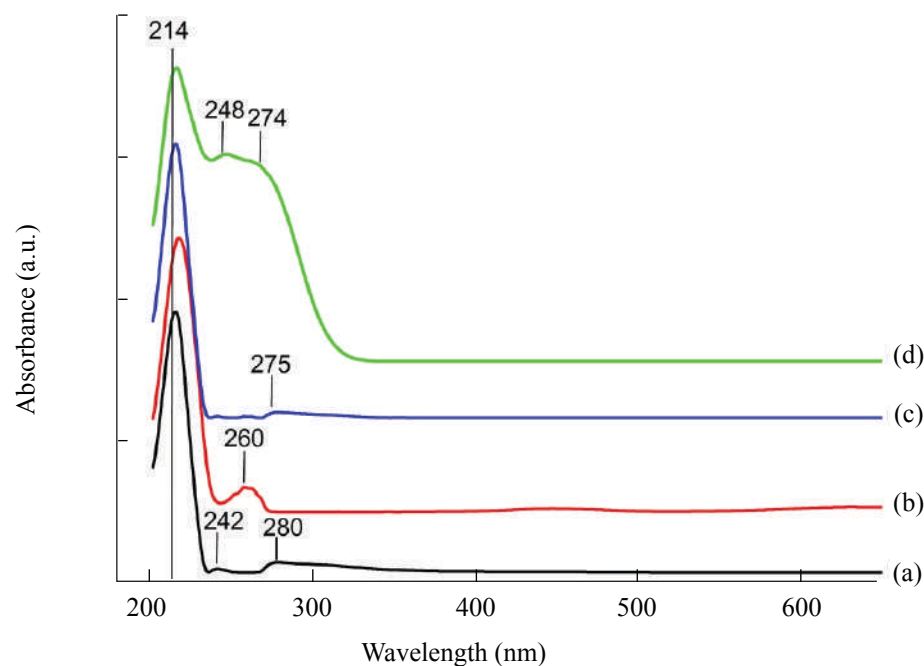


Figure 4. UV-Vis spectra of MeNKX-2 solid products: (a) CoNKX-2, (b) CrNKX-2, (c) ZrNKX-2 and (d) FeNKX-2.

SEM Analysis

The morphological properties of MeNKX-2 synthesized using different metal sources were studied using SEM technique (Figure 5). The SEM images showed that crystalline structure of MeNKX-2 could be obtained after 20 min of ionothermal heating. The data also showed that MeNKX-2 products have a unique morphology. The samples consisted of a novel rounded rectangle-like morphology with a rough surface, which is different from the hydrothermally and ionothermally synthesized NKX-2 crystals [11, 12]. Also, the introduction of different metals had no significant effect on the morphology of MeNKX-2.

EDX Measurement

The elemental analysis of MeNKX-2 samples was also performed using EDX analysis and the results were summarized in Table 1. The results showed that the transition metal cations had

been successfully incorporated into the NKX-2 framework but with different contents depending on the type of transition metal cations. Among four solids prepared, Fe^{3+} had the highest metal incorporated into the NKX-2 framework (Me/Al mass ratio = 0.0317) while Co^{2+} showed the lowest loading in the NKX-2 framework (Me/Al mass ratio = 0.0068). The elemental analysis was in line with the observation of UV-Vis spectroscopy results where FeNKX-2 gave the most intense signal at 240–280 nm whereas CoNKX-2 had the least intense signal at the same region.

Thermogravimetric Analysis (TGA)

Figure 6 shows the TG and DTG curves of the MeNKX-2 products. As can be seen, the curves displayed 2-step weight loss. The first step of weight loss at $<160^\circ\text{C}$ was due to the desorption of physically absorbed water. The second stage of weight loss at $160\text{--}427^\circ\text{C}$ was originated from the release of chemisorbed water [17]. Furthermore, weight gain also occurred after 427°C which can

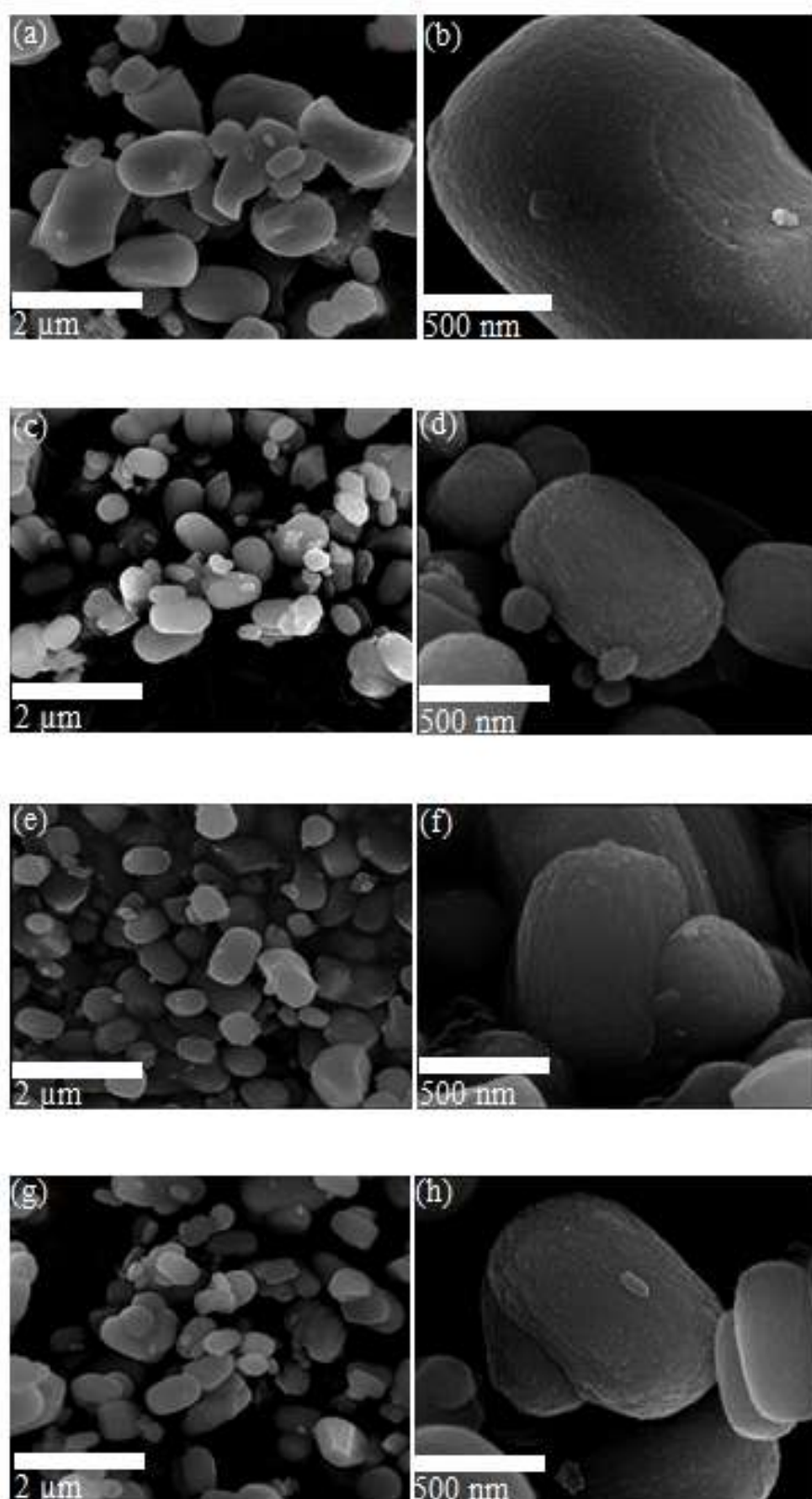


Figure 5. SEM images of (a, b) CoNKX-2, (c, d) CrNKX-2, (e, f) FeNKX-2 and (g, h) ZrNKX-2 solids under low and high magnifications.

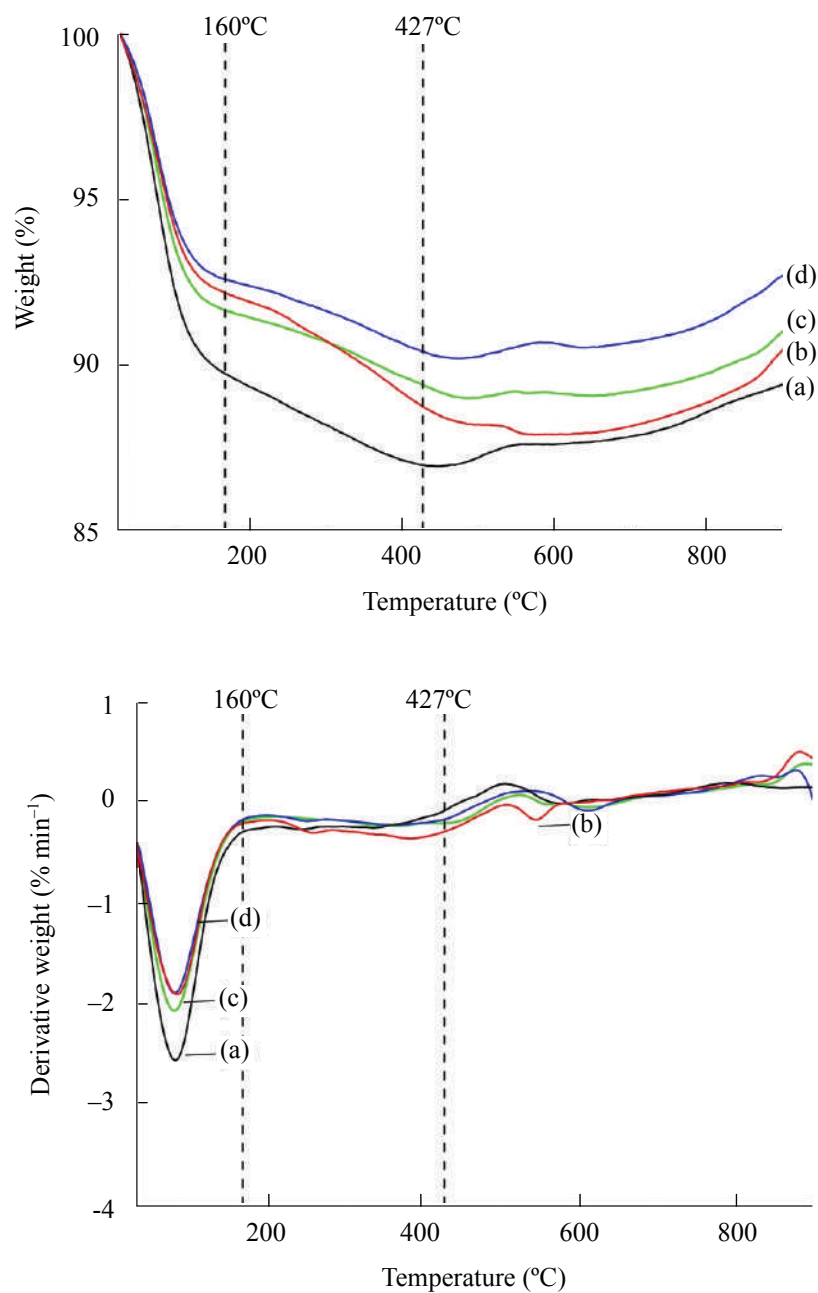


Figure 6. (Top) TG and (Bottom) DTG curves of (a) FeNKX-2, (b) ZrNKX-2, (c) CoNKX-2 and (d) CrNKX-2.

Table 1. Elemental analysis of MeNKX-2.

Sample	Me/Al mass ratio
CrNKX-2	0.0282
FeNKX-2	0.0317
ZrNKX-2	0.0259
CoNKX-2	0.0068

be explained by the formation of metal nitrides resulting from the reaction between the transition metal sources and the nitrogen gas atmosphere [18].

CONCLUSIONS

In conclusion, MeNKX-2 had been successfully synthesized via ionothermal approach using 1-benzyl-2,3-dimethylimidazolium chloride, [bdmim]Cl, ionic liquid as both solvent and structure directing agent. The synthesis conditions were investigated and were found that 20 min of heating was sufficient for crystallizing MeNKX-2. Also, an introduction of transition metals was found to be essential for the enhancement the crystallization rate of MeNKX-2. The synthesized MeNKX-2 was found to have novel rounded rectangle-like morphology where the morphology of the crystals was entirely different from the previous works. The EDX and UV-Vis spectroscopy studies also showed that different types of transition metals had different efficiency in the incorporation in the NKX-2 framework.

ACKNOWLEDGEMENT

The authors would like to acknowledge RUI (1001/PKIMIA/811264) research grant for financial support.

REFERENCES

1. Wilson, S.T., Lok, B.M., Messina, C.A., Cannan, T. R. and Flanigen, E. M. (1982) Aluminophosphate molecular sieves: a new class of microporous crystalline inorganic solids, *J. Am. Chem. Soc.*, **104**, 1146–1147.
2. Khoo, D.Y., Awala, H., Mintova, S. and Ng, E.-P. (2014) Synthesis of AlPO-5 with diol-substituted imidazolium-based organic template, *Micropor. Mesopor. Mater.*, **194**, 200–207.
3. Gopal, L., Lim, G.K., Ling, T.C., Adnan, R., Juan, J. C. and Ng, E.-P. (2016) Organotemplate-free hydrothermal synthesis of NaNKX-2 aluminophosphate basic catalyst, *Mater. Lett.*, **182**, 344–346.
4. Cooper, E.R., Andrews, C.D., Wheatley, P.S., Webb, P.B., Wormald, P. and Morris, R.E. (2004) Ionic liquids and eutectic mixtures as solvent and template in synthesis of zeolite analogues, *Nature*, **430**, 1012–1016.
5. Ma, H., Tian, Z., Xu, R., Wang, B., Wei, Y., Wang, L. Xu, Y., Zhang, W. and Lin, L. (2008) Effect of water on the ionothermal synthesis of molecular sieves, *J. Am. Chem. Soc.*, **130**, 8120–8121.
6. Pei R., Tian Z., Wei Y., Li K., Xu Y. and Wang L. (2010) Ionothermal synthesis of AlPO₄ molecular sieves in the presence of quaternary ammonium cation, *Mater. Lett.*, **64**, 2118–2121.
7. Pei R., Tian Z., Wei Y., Li K., Xu Y. and Wang L. (2010) Ionothermal synthesis of AlPO₄-34 molecular sieves using heterocyclic aromatic amine as the structure directing agent, *Mater. Lett.*, **64**, 2384–2387.
8. Chen, H., Chao, R., Na, B., Li, N., Xiang, S. and Guan, N. (2007) Effects of H₂O₂ and H₃PO₄ on synthesis of SAPO-41 and AlPO-41 molecular sieves using H₃PO₃ as the phosphorus source, *Chin. J. Catal.*, **28**, 501–503.
9. Ren X. -T., Li N., Cao J. -Q., Wang Z. -Y., Liu S. -Y. and Xiang S. -H. (2006) Hydroisomerization of n-decane over Pt/SAPO-41 catalyst, *Appl. Catal. A: Gen.*, **298**, 144–151.
10. Kong W., Dai W., Li N., Guan N. and Xiang S. (2009) A one-step route to SAPO-46 using H₃PO₃-containing gel and its application as the catalyst for methanol dehydration, *J. Mol. Catal. A: Chem.*, **308**, 127–133.
11. Li, N., Ma, Y., Xiang, S. and Guan, N. (2006) Capturing an aluminophosphate intermediate in the new route of synthesizing zeolite-like aluminophosphates, *Chem. Mater.*, **18**, 975–980.
12. Shi, Y., Zhang, X., Wang, L. and Liu, G. (2014) Ionothermal synthesis of aluminophosphate NKX-2, *Mater. Lett.*, **124**, 212–214.
13. Gómez-Hortigüela, L., Pérez-Pariente, J., Corà, F., Catlow, C. R. A. and Blasco, T. (2005) Structure-directing role of molecules containing benzyl rings in the synthesis of a large-pore aluminophosphate molecular sieve: An experimental and computational study, *J. Phys. Chem., B* **109**, 21539–21548.
14. Wei, W., Moulijn, J.A. and Mul, G. (2008) Effect of steaming of iron containing AlPO-5 on the structure

- and activity in N₂O decomposition, *Micropor. Mesopor. Mater.*, **112**, 193–201.
15. Weckhuysen, B.M., de Ridder, L. and Schoonedeheydt, R.A. (1993) A quantitative diffuse reflectance spectroscopy study of supported chromium catalysts, *J. Phys. Chem.*, **97**, 4756–4763.
 16. Chen, J., Zhang, H., Tomov, I.V., Ding, X. and Rentzepis, P.M. (2008) Photochemistry and electron transfer mechanism of transition metal oxalato complexes excited in the charge transfer band, *PNAS.*, **105**, 15235–15240.
 17. Ng, E.-P., Delmotte, L. and Mintova, S. (2008) Environmentally benign synthesis of nanosized aluminophosphate enhanced by microwave heating, *Green Chem.*, **10**, 1043–1048.
 18. Wang, Y., Wang, Y., Li, Y., Shi, H., Xu, Y., Qin, H., Li, X., Zuo, Y., Kang, S. and Cui, L. (2015) Simple synthesis of Zr-doped graphitic carbon nitride towards enhanced photocatalytic performance under simulated solar light irradiation, *Catal. Commun.*, **72**, 24–28.